Science on Form: Proceedings of the Second International Symposium for Science on Form,
Editor: S. Ishizaka, pp. 61–80.
Copyright © 1990 by KTK Scientific Publishers, Tokyo.

CONFOCAL MICROSCOPY OF BIOLOGICAL SPECIMENS

C. J. R. SHEPPARD[1] and C. J. COGSWELL[2]

[1]*Department of Engineering Science, University of Oxford, Parks Road, Oxford OX1 3PJ, United Kingdom**; [2]*Department of Biology, University of Oregon, Eugene, OR 97403, U.S.A.*

Key words: Confocal, Laser Scanning, Optical microscopy, 3-D imaging

Abstract. For imaging biological subjects, the confocal bright field method has some advantages over confocal fluorescence: axial resolution is greater, and images can be formed from unstained, living specimens. Techniques for imaging phase information (small changes in refractive index) are also possible and provide yet another realm of useful information about the specimen in addition to its absorption, transmission and reflection properties. Electronic or digital image enhancement techniques can be optimised to produce maximum visibility of detail for a human observer. Finally, optical sections from through-focus series can be combined to produce stereo pairs or stored with depth information and later imaged using a three-dimensional graphics representation.

INTRODUCTION

Optical microscopy is widely used for investigation of the structure of many categories of biological specimens. Its importance, only recently fully appreciated, stems from its ability to examine, in a non-damaging manner, samples which have undergone a minimum of preparation. In this way, specimen preparation artefacts can be avoided, in many cases it being possible to observe living biological subjects in their natural state. After a period of little significant instrumental development, optical microscopy is now being revolutionized by a range of techniques which can drastically improve the properties of the resultant images. These techniques in many cases are derived from a combination of scanning methods for image acquisition followed by computer image enhancement and display.

The scanning optical microscope has numerous advantages over the corresponding conventional instrument. Contrast and resolution can both be significantly improved, and subjects of appreciable depth can be imaged in three dimensions. The basic operation of the system is illustrated in Fig. 1. Light from a point source, in

*Now at: School of Physics, University of Sydney, NSW 2006, Australia.

This paper was presented at The Second International Symposium for Science on Form (October 19th–21st, 1988 at the University of Tsukuba, Japan).

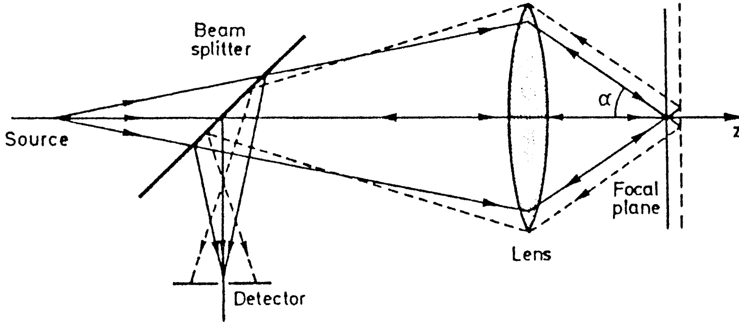

Fig. 1. Schematic diagram of the scanning optical microscope.

practice conveniently supplied by a laser, is focused by a microscope objective onto the object. The back-scattered light is collected by the same objective and focused onto a photodetector. The illuminating spot is scanned relative to the object in order to generate an image which can be displayed or stored for subsequent processing. Scanning can be achieved by mechanically moving the specimen or the objective lens. In both of these cases, the optical system is used completely on-axis. Alternatively, beam scanning can be employed.

Much of the advantage of scanning optical microscopy is that it can be used in a number of alternative and complementary imaging modes, including confocal and differential phase contrast configurations. In the confocal microscope, a small pinhole is placed in front of the photodetector. This has the effect that, in addition to the object being illuminated with a finely focused spot of light, the photodetector only detects light from the same region in three-dimensional space. In this configuration, resolution in a lateral direction is improved, but also light back-scattered from parts of the object above or below the focal plane of the system is defocused when it arrives at the pinhole and hence is detected very weakly. This produces a strong optical sectioning property (i.e. improved axial resolution) which allows three-dimensional structure to be investigated. In the differential phase contrast mode, a large area split-detector is employed to allow imaging of refractive index variations within the object or changes in its surface height. All the available imaging modes, because they generate the image in an electronic form, can be coupled to electronic enhancement and display devices.

IMPROVED AXIAL RESOLUTION: OPTICAL SECTIONING

Without a doubt, the best-known attribute of confocal optical microscopy for imaging biological subjects is the ability to extract information from one precise plane of focus of the specimen at a time, with virtually no blurring or distorting influences from portions of the object above or below the focal plane. This optical sectioning property is achieved in several confocal microscope arrangements including laser beam-scanning, specimen scanning, rotating Nipkow discs, slit scanning, etc., which are currently in use in research laboratories (see Boyde: 1988;

Sheppard: 1987, for review). Our microscope has been mechanically calibrated to focus through a semi-transparent specimen at incremental steps as fine as 0.1 micron which are small enough to record the axial information in the image. Several factors, inherent in this specific design, contribute to the improvement in depth resolution: (1) on-axis optics allow the aberrations of the system to be optimally minimized; (2) uniformity of illumination and detection sensitivity allow high degrees of contrast enhancement to be employed which maximizes visibility of fine structure; (3) low magnification (large field) scanning is possible with high N.A. objectives.

Figure 2 (a–d) shows a series of four reflected confocal optical sections from a 30 micron thick section of rat cerebellum fixed in paraformaldehyde/glutaraldehyde and stained for dendrites using a monoclonal antibody with horse radish peroxidase (HRP), diaminobenzidene (DAB) and osmium. The four images were obtained

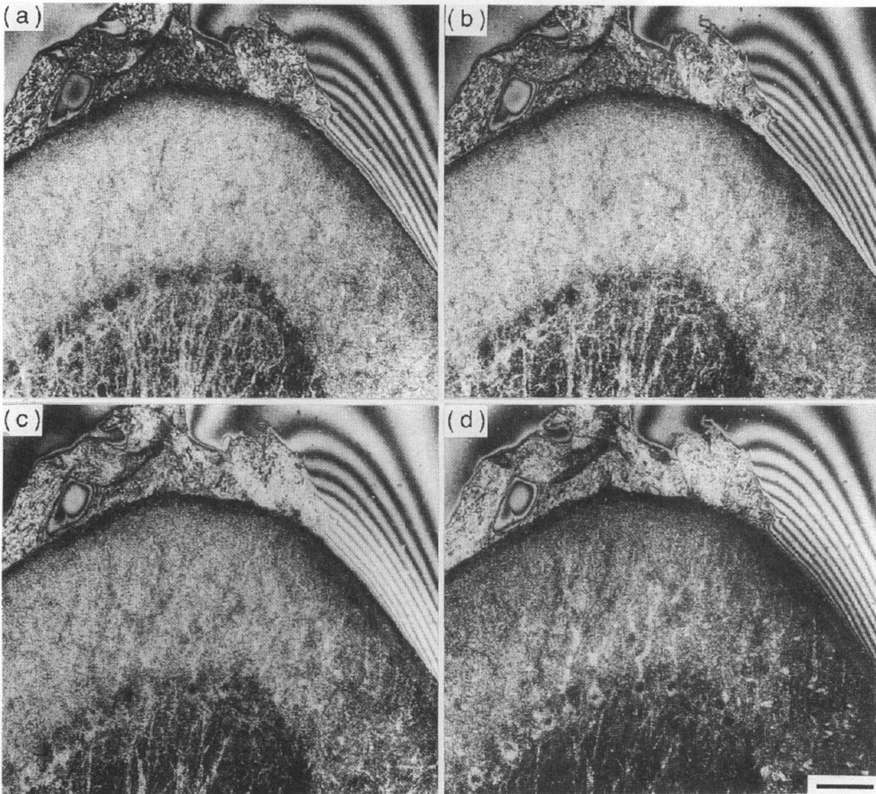

Fig. 2. Reflected confocal bright field optical sections at 1 micron increments of focus from a 30 micron thick section of rat cerebellum. In (a) and (b), unstained axons are clearly visible in the lower regions of the images (granule cell layer) under the semicircular row of Purkinje cells. In (d), which is focused 3 microns below (a), the axons are no longer visible but now dendrites can be seen to radiate upwards into the molecular layer. Scale=50 microns. (Preparation courtesy of Dr. R. A. J. McIlhinney, University of Oxford)

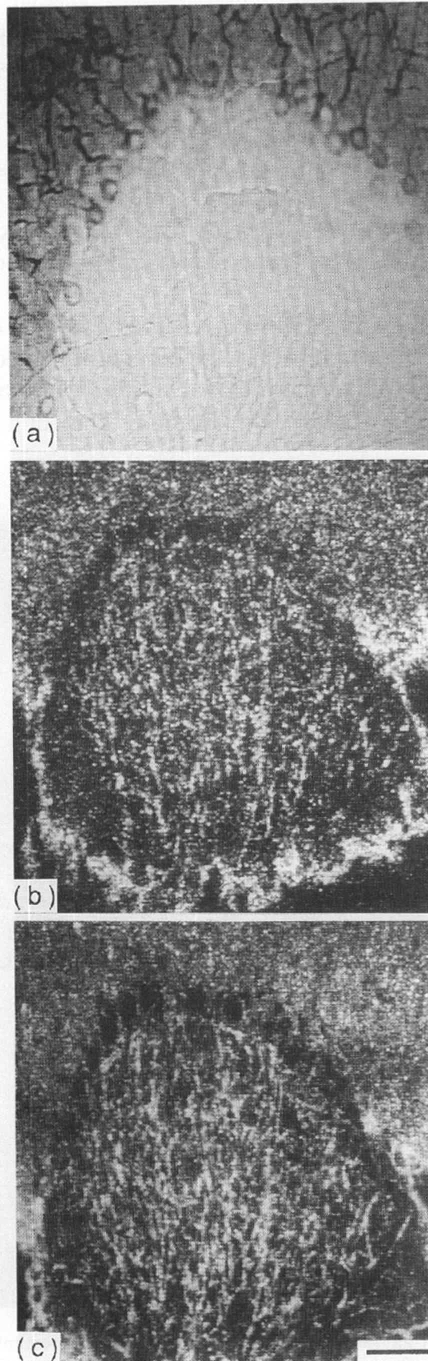

Fig. 3. Rat cerebellum, 30 micron thick section. (a) transmitted conventional bright field image showing darkly stained dendrites radiating upwards into the molecular layer. Axons in the central granule cell layer cannot be visualized due to blurring effects from out-of-focus planes. (b) reflected confocal bright field image of exactly the same region and plane of focus. Now unstained axons in the granule cell region are visible. (c) extended focus technique to give increased depth-of-field over the reflected confocal image, yet avoiding blurring effects from out-of-focus planes. Scale=40 microns.

from successive planes of focus at 1 micron intervals. Variations in microstructure in depth are clearly delineated. Figure 3b shows an enlarged view of the Purkinje cell region at the boundary between the molecular and granule cell layers using the same reflected confocal configuration. Unstained axons are clearly visible in the granule cell layer (centre of field). For comparison, Fig. 3a is the identical sample and plane of focus, only now the light has been transmitted through the sample and an image formed using a large area (non-confocal) detector. This image is equivalent to that formed in a conventional transmitted bright field microscope. Although the stained dendrites are clearly visible in the region above the line of Purkinje cells, the central portion of the micrograph is comprised of so much out-of-focus information superimposed on the focused image that the axons virtually disappear into the background haze.

Although precise imaging of a very narrow thickness in depth has a multitude of useful applications, the ability to image accurately a larger thickness in the axial dimension may also be extremely valuable. To achieve this increased depth-of-focus, the microscope has been equipped with a piezo-controlled objective focusing system which allows the microscope to scan through a user-specified depth interval while simultaneously scanning in the *x-y* plane. The brightness response from each spot as the microscope scans in depth is averaged to form an image comprised of several sharply focused planes superimposed. The image represents a projection of the object in the axial direction. This extended focus technique (Sheppard *et al.*: 1983) is illustrated in Fig. 3c. Now the geometry in depth of the axons is clearly visible as compared to the bright field image, Fig. 3b.

ADDITIONAL OPTICAL CONFIGURATIONS FOR SCANNING MICROSCOPY

Although confocal microscope systems utilizing fluorescence (Cox: 1984; Brakenhoff *et al.*: 1986; Carlsson *et al.*: 1985; Wijnaendts van Resandt *et al.*: 1985) or reflected bright field (Boyde: 1985) have begun to make an impact in many biological and medical disciplines, the true power of the instrument may prove to be in its potential for obtaining unique information from biological subjects that has been previously impossible to obtain with conventional light microscope systems. The scanning optical microscope can be designed in such a way that a variety of optical techniques can be employed at the operator's discretion. One such technique is the ability to scan the specimen in depth while at the same time scanning across a single lateral line (as viewed from the top of the object). This we refer to as *x-z* imaging and it is made mechanically and optically possible by the same piezo-controlled objective focusing described above for the extended focus technique. The *x-z* imaging technique has the effect of looking at a plane of focus through the specimen from a side or lateral view. Figure 4a is an enlarged region of the same rat brain viewed from the top (*x-y* image) using the confocal reflected bright field configuration. The *x-z* image, Fig. 4b, was created by selecting a horizontal line through the centre of the *x-y* image and scanning this line over a 16 micron distance in depth (along the *z* axis). The *x-z* image clearly shows the variations in surface height across the specimen (bright peaks) as well as the location of a Purkinje cell in

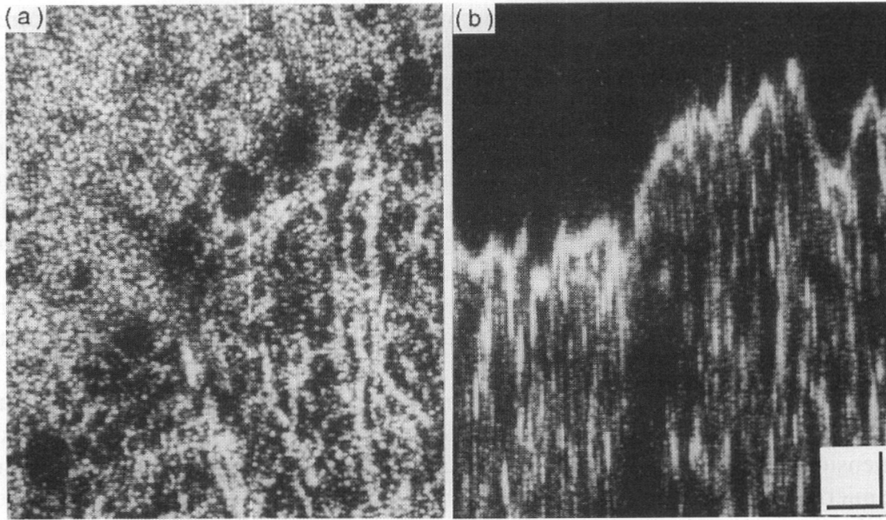

Fig. 4. (a) enlarged view of rat cerebellum, reflected confocal bright field. Dark circles are Purkinje cells. (b) *x-z* image created by scanning in depth (*z*-axis) across a single horizontal line through the centre of image (a). This produces a side view image in which variations in specimen height appear as bright peaks while the location of a Purkinje cell below the surface is visible as a dark hole. Note: horizontal scale=20 microns (both images), vertical scale in image (b)=1.5 microns which produces an exaggerated depth appearance.

depth (dark hole in centre). Further development to improve resolution and minimize distortions in this technique should lead to an extremely useful tool for retrieving three-dimensional structural information in a wide variety of biological subjects.

Yet another optical configuration of the scanning microscope provides the opportunity for retrieval of information regarding slight changes in refractive index within a biological subject or between the subject and its surrounding medium. This system, called differential phase contrast, is able to detect refraction effects at edges (refractive index boundaries) which results in phase information being imaged in addition to the amplitude information (i.e. absorption) characteristic of conventional bright field microscopes (Sheppard & Hamilton: 1984). These refraction effects are dependent on the angle of incidence of the illuminating beam and the orientation of the edge (refractive index boundary) in the sample. Two images, each produced by an opposing half aperture detector, will appear different wherever a component of an edge boundary parallel to the half aperture division has produced a tilt in the resulting transmitted beams. When these two images are subtracted (and an offset midtone grey signal added to improve visibility) the resulting image shows alternately highlights and shadows along refractive index boundaries. Figure 5a is a human buccal epithelial cell imaged with the differential phase contrast technique in transmission. A large split-detector has been used to detect the signal from each half of the illuminating aperture and the resulting signals have been electronically subtracted.

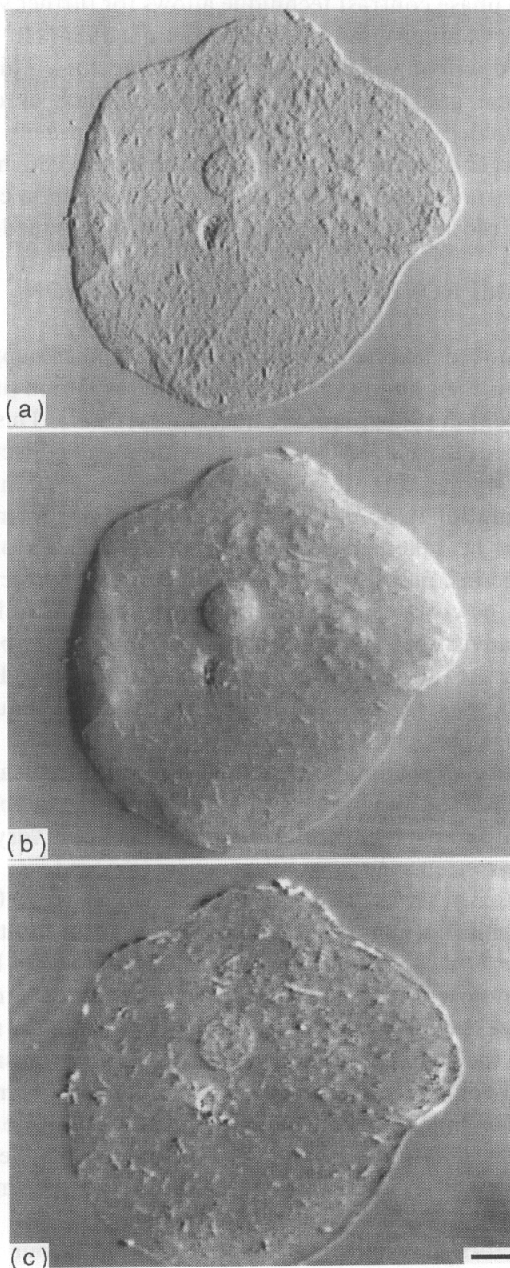

Fig. 5. Human buccal epithelial cell, unstained. (a) transmitted differential phase contrast (non-confocal) with large aperture split-detector. (b) same as (a) but with a circular obstruction in front of the detector. (c) same as (b) but with a larger circular mask. Scale=0.75 microns.

This differential phase contrast technique allows for further variations employing different detector configurations (Hamilton *et al.*: 1984). In Fig. 5b a circular mask has been placed in front of the half aperture detectors. This has the effect of enhancing weak phase gradients so that phenomena such as changes in object thickness (as in the folded left side of the cell) become apparent. Figure 5c, on the other hand, uses a larger diameter obscuring mask to enhance high spatial frequency information. Cytoplasmic inclusions as well as surface bacteria can now be clearly seen while thickness information has been almost totally subdued.

IMPROVED LATERAL RESOLUTION

An often overlooked feature of scanning optical microscope systems which utilize coherent light is their ability to improve lateral resolution (in the *x-y* plane) as well as resolution in depth (Sheppard & Choundhury: 1977). This is due to the fact that the object is effectively imaged using both incident and collected light, and may provide as much as 1.4 times the lateral resolution of a conventional microscope. To obtain improved resolution in practice, however, several factors must be considered and great care must be taken in setting up the system. In order to minimize aberrations, it is of course necessary to use an objective of correct tube length and, ideally, one that can be corrected for coverglass thickness as well. In addition, we have found that it is advisable to correct for residual aberrations by using correction lenses or by adjusting the tube length for optimum performance. Even then, the fact that the system is focused through different thicknesses of mounting medium at different depth settings needs to be considered.

Resolution is also dependent on pinhole size, and critically dependent on alignment of the pinhole on the optic axis. All of the these factors affect the axial resolution as well, and in particular we have found that it is very sensitive to even small amounts of aberration.

Figure 6 (a–c) is a series of three optical sections, at 0.4 micron focus increments, of late mitotic anaphase in endosperm tissue of the African globe (blood) lily, *Haemanthus katherinae*. The microtubule bundles have been labeled with 15–20 nm immuno-gold which is readily detected by the confocal reflected optics used to produce the left-hand images. For comparison, the right-hand images in Fig. 6 (a–c) show the same three increments of focus in transmitted differential phase contrast (non-confocal) and appear similar to the Nomarski differential interference contrast technique of conventional microscopy. Here the chromosomes are visible as well as the microtubule bundles of the mitotic spindle, owing to the fact that the images represent a much thicker region of the specimen and therefore poorer depth resolution than the reflected confocal images.

To illustrate factors that improve lateral resolution in our reflected confocal bright field design, a region out of the centre of the cell was imaged at 9,000 diameters magnification. Figure 7a shows a few microtubule bundles imaged with a 100×, 1.3 N.A., oil immersion lens and a 10 micron diameter pinhole in front of the detector. Changing to a 2.5 micron detector pinhole, Fig. 7b, gives an improvement in lateral resolution which is in keeping with predictions based on theory (Wilson & Carlini: 1987). On the other hand, Fig. 7c shows the effects of using an objective that

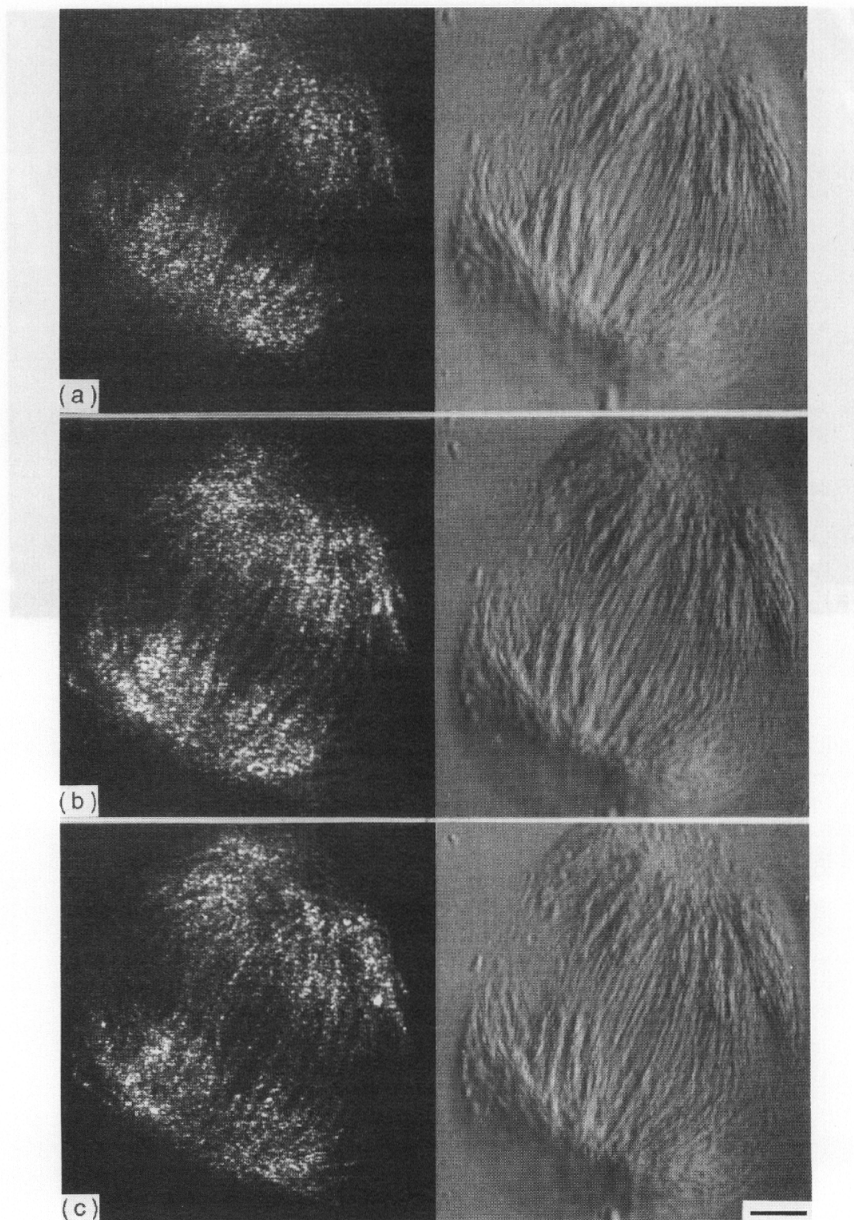

Fig. 6. Mitotic anaphase in endosperm tissue of the African blood lily, ***Haemanthus katherinae***. Microtubule bundles labeled with 15–20 nm immunogold. In (a–c), pairs of images were made using confocal reflected (left) and transmitted differential phase contrast (right) at focus increments of 0.4 microns between each pair. Microtubule bundles can be precisely located in depth in the left images, whereas several planes of microtubules and chromosomes are superimposed in the non-confocal differential phase images. Scale=10 microns.

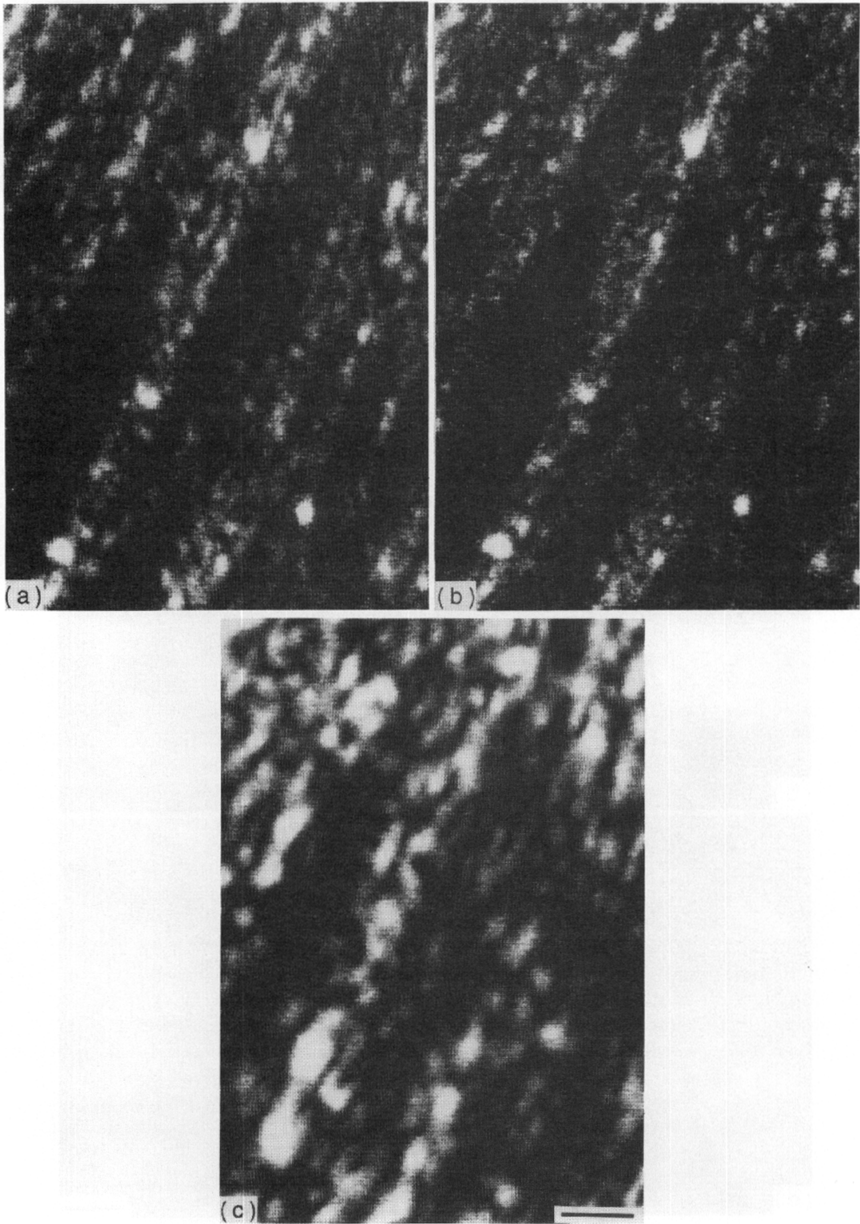

Fig. 7. Enlarged view of *Haemanthus* microtubule bundles using confocal reflected bright field. In (a), a 10 micron pinhole was placed in front of the detector. (b) changing to a 2.5 micron detector pinhole shows an improvement in lateral resoluton. (c) image of the same region using the same objective with its tube length correcting lens removed. Aberrations present in this configuration greatly reduce resolution. Scale=1.5 microns. (Preparation courtesy of Dr. J. Mole-Bajer and Dr. A. S. Bajer, University of Oregon).

has not been precisely corrected for tube length. Here, aberrations so greatly degrade the resulting image that microtubule bundles are virtually impossible to distinguish. This emphasizes the fact that great care is necessary in correction of the optics in order to obtain optimum performance.

IMAGE ENHANCEMENT AND DISPLAY

Even though a variety of optical configurations may initially provide a wide range of potentially useful information about a given biological subject, it is always imperative to consider how the final image should be displayed to maximize the visual information available to a human observer. A host of analogue and digital image processing techniques are commonly in use in conventional biological microscopy (Moss: 1988). However, the special properties of confocal scanning optical microscopes, and particularly our design which uses on-axis coherent light, produce images which lend themselves very well to a few specific image enhancement and display techniques.

Because a confocal microscope can produce a series of optical sections through an object, each representing a precise plane of focus, it has become standard practice to display these through-focus series as stereo pairs. Figure 8 is a computer-generated stereo pair of four rat brain optical sections similar to Fig. 3b, but at twice the magnification. The algorithm to create the stereo pair compares each point in an image to the values in the corresponding *x-y* locations in each section of a through-focus series. To form the left half of the stereo pair, it stores the maximum (brightest) value that it found at each *x-y* location during the through-focus comparison. This we refer to as an autofocus image (Cox & Sheppard: 1984) and, although it too produces a projection of the object, it is slightly different from the extended focus technique previously described since it records the maximum signal in depth rather than an average of that point for all planes of focus. To form the

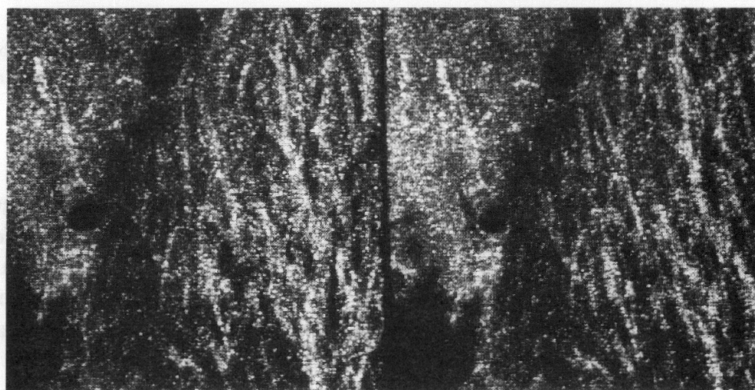

Fig. 8. Stereo pair from four rat cerebellum confocal optical sections, similar to Fig. 3b, but at twice the magnification. Images were at 0.5 micron intervals in depth. Location of axons in depth in the granule cell layer (right portion of image) is clearly discernible.

right half of the stereo pair, the algorithm also displays the maximum values but displaces them successively one pixel to the right for each focus step occurring between the plane containing the point of maximum brightness and the top optical section in the series.

Sometimes the human visual system can more clearly resolve dark points or lines on a light background rather than bright points on a dark field. Figure 9 is a stereo pair produced from a series of contrast-reversed confocal images (as compared to Fig. 6) of the *Haemanthus* mitotic cell. Other techniques for displaying stereo pairs include colouring each half of the pair a different primary colour (such as red and green) and super-imposing the two images which are then viewed through red-green spectacles. One interesting observation with this technique on our colour display monitor is that the stereo effect can be reversed in depth by simply looking at the image with the opposite colour filter over each eye (i.e. just turning the red-green spectacles around). This has the effect of looking up through the bottom of the sample and also gives a stereo image that appears to emerge outward from the plane of the colour monitor screen.

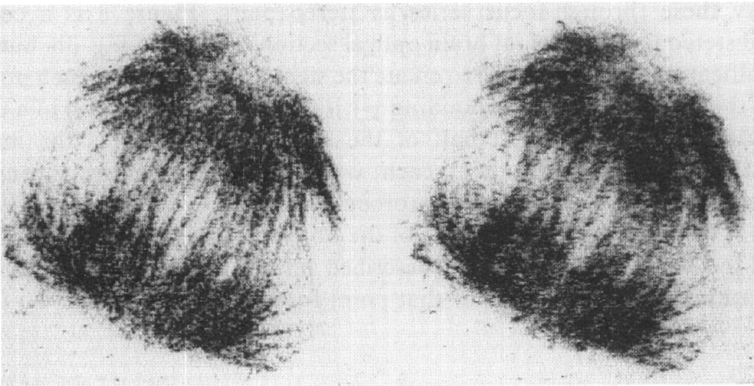

Fig. 9. Stereo pair of mitotic anaphase in *Haemanthus* at similar magnification to Fig. 6 but with contrast reduced to improve visibility of microtubule bundles in depth. Eight optical sections at 0.2 micron focus steps were used to create the stereo pair.

To illustrate some other techniques for enhancing and displaying images using our system, a through-focus series of images was made of a living *Tradescantia* stamen hair cell, mounted in water. Images were stored of optical sections taken at 2 micron intervals through the 30 micron thick cell. Figure 10 (a–h) shows a portion of the through-focus series with the reflected confocal bright field images appearing on the left half of the figure and transmitted differential phase contrast images appearing on the right. The reflected confocal images clearly delineate the cytoplasmic channels (running through the centre of the cell and along the edge of the cell wall) which contain numerous mitochondria, plastids and other cytoplasmic inclusions that appear as brightly reflective spots. The dark regions surrounding the channels

are vacuoles containing water and dissolved mineral solutes which reflect very little of the incident illumination.

Figure 11 (a–d) shows a higher magnification view of the upper right portion of the cell at two planes of focus, 2 microns apart, with the left images made using the standard reflected confocal configuration and the right images produced by electronically differentiating the confocal analogue signal. This edge-enhancement technique was employed to assist the human observer in distinguishing meaningful cell surface structure (striations) from the speckle pattern that is commonly present in high magnification images produced using coherent light.

Instead of enhancing the visibility of the meaningful information relative to the speckle, it is also possible to reduce the effect of the speckle itself. For example, the extended focus method averages over a finite depth of the specimen and the contrast of the speckle pattern is reduced, as is apparent from Fig. 3c. The autofocus method behaves in a similar fashion, but is not so effective in this way (Fig. 8). Other possibilities for reducing the effects of speckle include averaging over two planes of polarization or over a range of wavelengths. Perhaps the best solution would be to employ the digital reconstruction methods of diffraction tomography, for example, those based on the Rytov approximation (Kaveh & Soumekh: 1987).

Figure 12 is a stereo pair of seven planes of focus from the reflected confocal bright field series shown in Fig. 10 (a–h). As described above, the left image of the stereo pair is formed by recording the maximum brightness signal for each x-y location in the through-focus series. While creating this autofocus image, Fig. 13a, an additional algorithm produces a second image called a surface profile, Fig. 13b. This technique records the position of the maximum signal in depth and displays this information as a grey scale map, where the further the maximum occurs in the focus series, the darker it appears in the surface profile image. These two images can subsequently be used to provide input data for a large number of possible three-dimensional graphics display routines. One such algorithm was used to produce an isometric projection of the stamen hair cell, Fig. 13c, with the surface brightness values taken from the autofocus image and the correct position in depth calculated from the surface profile image.

CONCLUSION

Although confocal fluorescence microscopy appears to have established itself as an important technique for obtaining information regarding three-dimensional structure of appropriately stained biological subjects, it is by no means the only confocal microscopy system which has application to the field of biological imaging. The confocal bright field method even has some advantages over confocal fluorescence: axial resolution is greater, and images can be formed from unstained, living specimens. Techniques for imaging phase information (small changes in refractive index) are also possible and provide yet another realm of useful information about the specimen in addition to its absorption, transmission and reflection properties. When coupled to devices which can provide electronic or digital image enhancement, these techniques can be optimised to produce maximum visibility of detail for a human observer. Finally, optical sections from through-focus series can be

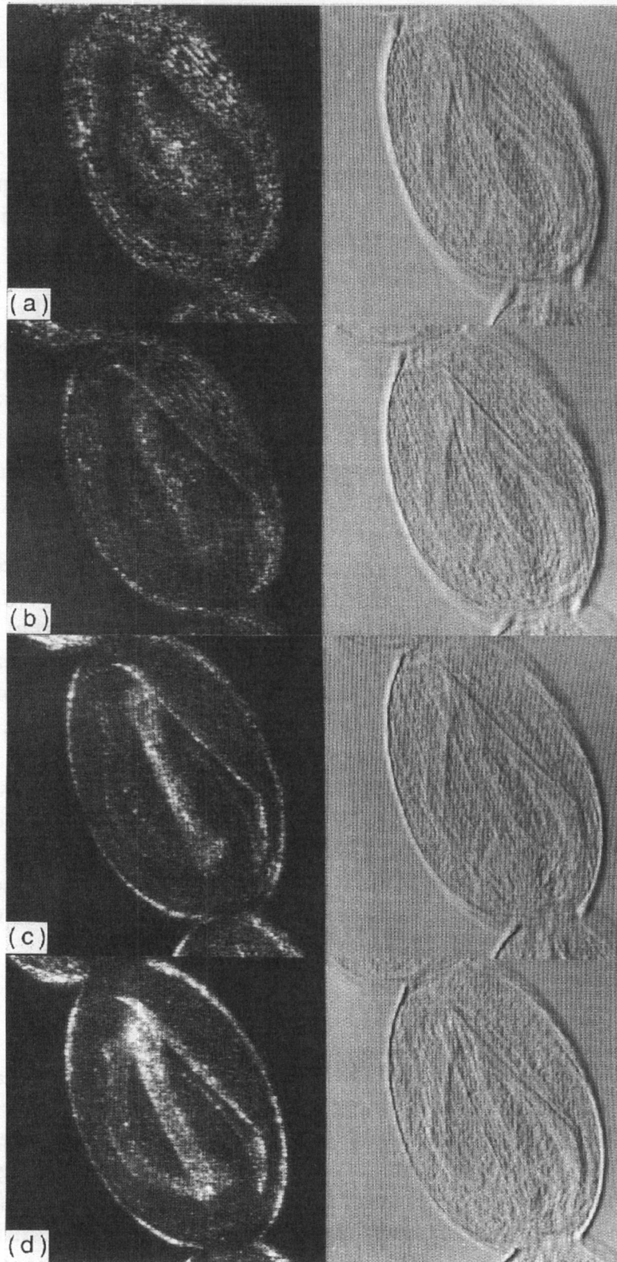

Fig. 10. Living stamen hair cell from a flower of *Tradescantia* imaged with confocal reflected bright field (left) and transmitted differential phase contrast (right). (a– h) are a through-focus series at 2 micron depth increments. Scale=20 microns.

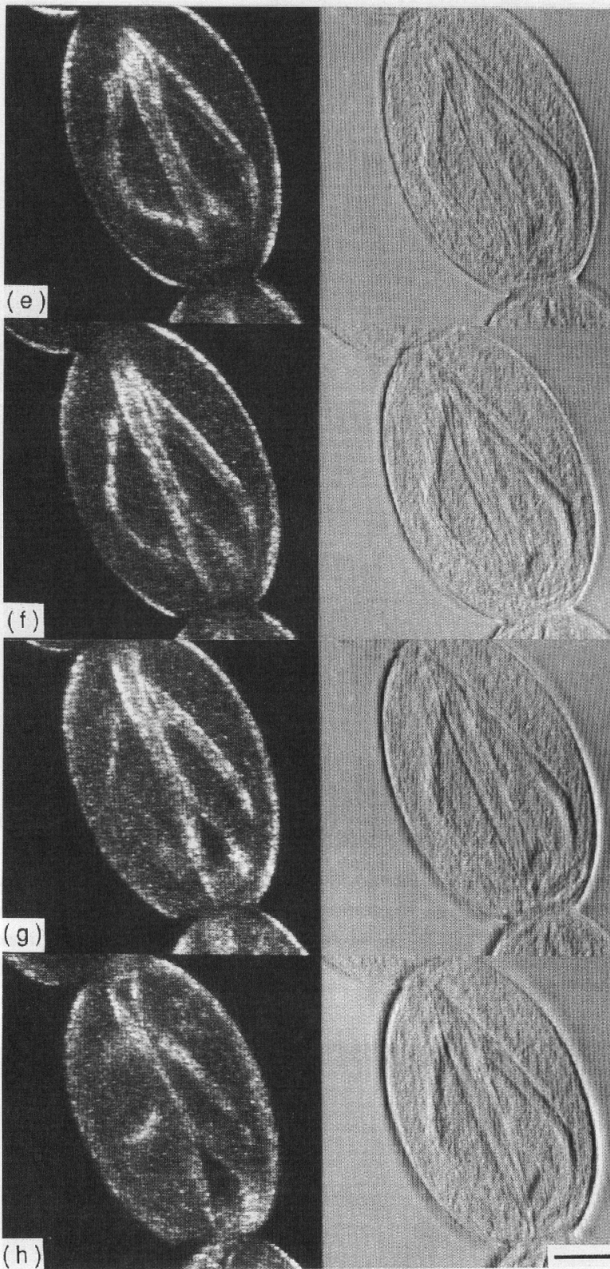

Fig. 10. (continued).

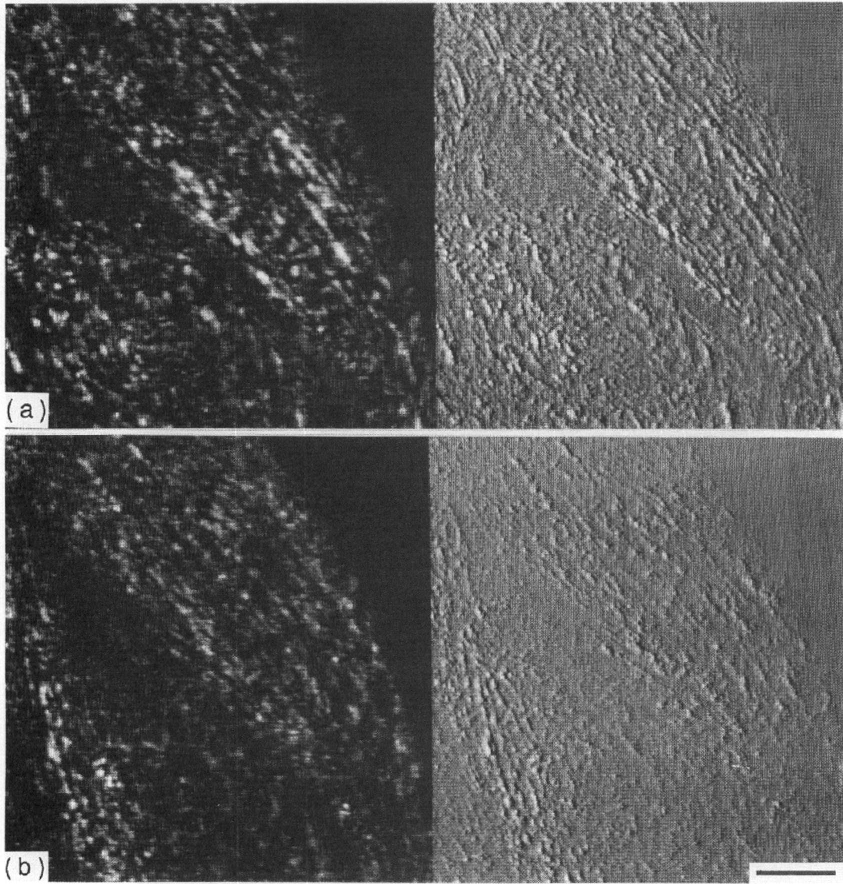

Fig. 11. Enlarged view of upper right portion of *Tradescantia* stamen hair cell (see Fig. 10a). Left images are confocal reflected bring field. Right images have been electronically differentiated to reduce the distracting speckle appearance of the standard confocal configuration, thus making cell surface striations more visible to a human observer. (a) is focused at the top surface of the cell and (b) is focused 2 microns below. Scale=10 microns.

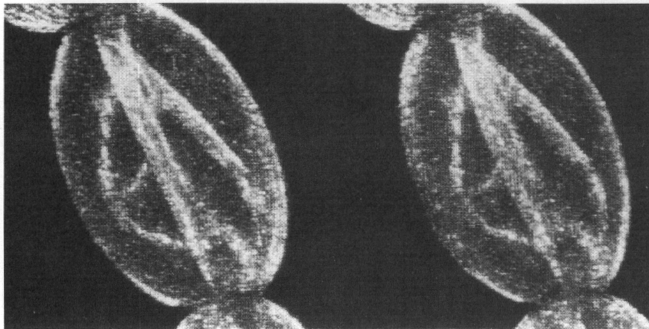

Fig. 12. Stereo pair of seven planes of focus from the *Tradescantia* confocal reflected bright field series illustrated in Fig. 10 (b–h). Location of the brightly reflecting cytoplasmic channels in depth can be clearly distinguished from the surrounding, darker-appearing vacuoles.

Fig. 13. *Tradescantia* stamen hair cell. (a) autofocus image created in the same way as the left half of the stereo pair in Fig. 12. (b) surface profile image where a grey scale has been used to code the significant bits in the image according to their location in depth (light grey=top, dark grey=bottom of cell). (c) isometric projection using information from both (a) and (b).

combined to produce stereo pairs or stored with their attendant depth information and later imaged using a three-dimensional graphics representation.

REFERENCES

Boyde, A. (1988): Confocal optical microscopy. *Microsc. and Analysis*, **Jan**: 7–13.

Boyde, A. (1985): The tandem scanning reflected light microscope: Part 2—Pre-Micro '84 applications at UCL. *Proc. Roy. Microsc. Soc.*, **20**: 121–139.

Carlsson, K., Danielsson, P. E., Lenz, R., Liljeborg, A., Majlof, L., and Aslund, N. (1985): Three-dimensional microscopy using a confocal laser scanning microscope. *Opt. Lett.*, **10**: 53–55.

Cox, I. J. (1984): Scanning optical fluorescence microscopy. *J. Microsc.*, **133**: 149.

Cox, I. J. and Sheppard, C. J. R. (1983): Digital image processing of confocal images. *Image and Vision Computing*, **1**: 52–56.

Hamilton, D. K., Sheppard, C. J. R., and Wilson, T. (1984): Improved imaging of phase gradients in scanning optical microscopy. *J. Microsc.*, **135**: 275–286.

Hamilton, D. K. and Sheppard, C. J. R. (1984): Differential phase contrast in scanning optical microscopy. *J. Microsc.*, **133**: 27–39.

Kaveh, M. and Soumekh, M. (1987): Computer-assisted diffraction tomography. *Image Recovery: Theory and Application*. [ed. H. Stark. Academic Press.]: 369–413.

Moss, V. A. (1988): Image processing and image analysis. *Proc. Royal Microsc. Soc.*, **23**: 83–88.
Sheppard, C. J. R. (1987): Scanning optical microscopy. *Advances in Optical and Electron Microscopy*, **10**: 1–98.
Sheppard, C. J. R., Hamilton, D. K., and Cox, I. J. (1983): Optical microscopy with extended depth of field. *Proc. R. Soc. Lond.*, **A387**: 171–186.
Sheppard, C. J. R. and Choudhury, A. (1977): Image formation in the scanning microscope. *Optica Acta*, **24**: 1051–1073.
Wijnaendts van Resandt, R. W., Marsman, H. J. B., Kaplan, R., Davoust, J., Stelzer, E. H. K., and Striker, R. (1985): Optical fluorescence microscopy in three dimensions: microtomoscopy. *J. Microsc.*, **138**: 29–34.
Wilson, T. and Carlini, A. R. (1987): Size of the detector in confocal imaging systems. *Optics Letts.*, **12**: 227–229.

DISCUSSION

Q. Where does the confocal resolution factor 1.4 come from? (Fujita, S.)

A. Near the focus the intensity in the image of a point in a conventional system can be expanded as a power series in cylindrical coordinates

$$I(r, z) = 1 - ar^2 - bz^2$$

where a and b are constants. This is true for any circularly symmetric system. In a confocal system the intensity is squared, giving

$$\begin{aligned} I(r, z) &= 1 - 2ar^2 - 2bz^2 + \ldots\ldots \\ &= 1 - a(\sqrt{2}r)^2 - b(\sqrt{2}z)^2. \end{aligned}$$

So resolution in both r and z directions is increased by $\sqrt{2}=1.414$ for a point object. Different resolution improvement factors are applicable for other resolution criteria, but these are usually in the range from 1 to 2.

Q1. You mentioned you can do computer generated holograms. Is this a simpler way than doing a hologram directly and what is the state of holography with biological specimen? Does it deliver good 3D information?

Q2. Is the scanning speed of a mechanical scanner generally less than that of the optical scanners?

Q3. Can you summarize the advantages of mechanical scanning compared to optical scanning?
Does your scanner work in resonance?
—So the scanning speed is independent of the mass of the scanned specimen. (Niemann, B.)

A1. In confocal microscopy we produce a complete 3D image. I proposed making a hologram of this 3D data by calculating the hologram in a computer and then printing in some way, say by electron beam lithography. So we make a hologram of the *intensity* data. This is of course not the same as making a

hologram directly. It is merely a way of displaying the 3D image. Note that this method can also be used with confocal fluorescence. I am not sure of the current status of direct holographic microscopy, but it has the disadvantage of being coherent imaging, so that speckle may be a problem and spatial frequency bandwidth is half that of confocal. A hologram also does not contain a complete 3D data set.

A2. The line scan of our object scan system operates at about 100 Hz for 2 mm amplitude. Commercial beam scanning instruments based on galvo scanners are not significantly faster. For smaller scan amplitudes (i.e. higher magnification) we have experimented with speeds up to 1000 Hz, but sound generation can be a problem. We work above the resonant frequency. Scan speed is fixed by the scan generator, but there is a phase lag which depends on the specimen mass.

A3. The advantages of mechanical object scanning are that, because the optics is used on axis,

a) imaging properties are constant over the whole field.
b) aberrations can thus be optimized.
c) illumination and detection sensitivity are constant over the field allowing high measurement accuracy.

Q. Once the image has been processed into a 3-D surface in the computer it is relatively straight forward to use *motion* (such as rotation) to give visual cues to the viewer of the 3-D nature of 2-D projections (as was mentioned by Professor Brakenhoff). Have you tried using "moving images" to display the 3-D surfaces? (Walton, O.)

A. Yes, I agree that once you have the image in the form of a surface it is possible to rotate the image in real time. We have not done this at present. Note that for a computer 3D image (a 3D array of grey levels) the information content is so high that rotation in real time is not at present feasible with ordinary computers. How easy it is to convert the complete image into the form of a surface, or in some other way reduce the amount of data, depends on the specimen.

Q. Do you think that the lens manufacturers will design new lenses specifically for confocal microscopy? (Howard, C. V.)

A. For on-axis scanning it is possible to design lenses for improved performance. We have designed a lens of numerical aperture 0.95 (dry) with a working distance of 1 mm, for example. Similarly it may be possible to design lenses with higher NA or to operate at shorter wavelengths than is usually possible. For beam-scanning systems there is not so much to be gained. I don't know whether lens manufactures are considering special lenses.

Q1. Why do you use red and green for stereo pair display?

Q2. What is the standard required time to make a frame of image of (say) metal

surface?

Q3. What is the practical height measurable (for example) in 500 μm$\times$500 μm field of view? (Kimura, A.)

A1. Red and green are commonly used for stereo display in Europe. The bandwidth of the filters are quite large so the display can be observed using red/blue spectacles.

A2. Our microscope operates at 100 Hz for the line scan. Most of the images shown were 256$\times$256 pixels, which thus take less than 3 seconds to form. For high resolution analogue display we use a scan time of 30 seconds. Of course 3 dimensional scanning takes longer.

A3. Using confocal microscopy surface height can be measured with a sensitivity of about 50 nm. Sensitivity can be improved by using confocal interferace methods. Our system has a sensitivity of 1 nm, but it is possible to achieve sub-ångstrom sensitivity. Note that we must distinguish between sensitivity and resolution—axial resolution is about 400 nm.

Q. In one of your slides you said your sample, microtubules if I remember correctly, was stained with gold particles. Was the staining absolutely necessary? What is the size limit, in confocal microscopy, beyond which detection requires staining? I ask this because I know that microtubules can be seen without staining under a dark-field microscope. (Kinosita, K.)

A. We did not try to image the microtubules without gold staining and so cannot state with any certainty what images of such a specimen would look like. The advantage of gold staining is that the gold particles reflect light which is then located in space by the imaging process. Without staining the detected light has been back-scattered primarily by refractive index variations in the object. A confocal microscope behaves as a differential imaging system for axial information and hence such index variations are imaged. As described in this paper such images might exhibit speckle, but also as described the speckle may be reduced by a number of alternative methods. These topics are the subject of further research.